

Linear scaling calculation for optical-absorption spectra of large hydrogenated silicon nanocrystallites

Shintaro Nomura, Toshiaki Iitaka, Xinwei Zhao, Takuo Sugano, and Yoshinobu Aoyagi
The Institute of Physical and Chemical Research, Hirosawa, Wako-shi, Saitama, Japan

(Received 24 April 1997)

A linear scaling calculation of the optical-absorption spectra is performed for hydrogenated silicon nanocrystallites up to 13 464 Si atoms. The calculation is performed in real space and is based on a time-dependent representation of the linear-response function. The empirical pseudopotential method is used for potentials of silicon and hydrogen atoms. The peaks in higher excited states in the ultraviolet region of the calculated absorption spectra are shown to shift to higher energy with a decrease in size. [S0163-1829(97)52232-6]

Photoluminescence measurements near the band gap have been investigated for experimental verifications of the quantum confinement effects in Si nanocrystallites.¹ Many of reported photoluminescence spectra show peaks between 1.5 and 2.0 eV depending on the size, which is explained by the recombination of the lowest electron-hole pairs in Si nanocrystallites.²⁻⁴ The peak positions of the observed photoluminescence vary, however, probably because of the oxidized layer on the surface or impurities depending on sample preparation procedures, which prevents quantitative comparison with theoretical calculations.

By contrast, the ultraviolet and visible absorption spectra are considered to be less affected by oxygen or other impurity atoms. The absorption spectrum measurements have been investigated up to about 6 eV.^{3,5} Since the advent of high intensity synchrotron orbital radiation (SOR), ultraviolet absorption measurements have become a useful tool for experimental clarification of the quantum confinement effects for higher excited states. The optical-absorption measurement of higher photon energy is feasible with SOR, which allows direct observation of optical transitions, such as X_4 to X_1 or L'_3 to L_3 critical points in bulk Si. The size dependence of these transitions is one of the most important signatures of the quantum confinement effects in Si nanocrystallite samples.

The transitions to higher excited states are also important for understanding the photoluminescence spectra of Si nanocrystallites in amorphous Si, which showed peaks at around 3 eV.^{6,7}

There are, however, only a few reports on the optical-absorption spectrum of Si nanocrystallites. A pseudopotential-based Chebyshev polynomial expansion method^{8,9} was used to calculate the imaginary part of the dielectric function of $\text{Si}_{1035}\text{H}_{452}$. Size dependence of the imaginary part of the dielectric function was studied by a linear combination of an atomic-orbitals-based tight-binding method up to $\text{Si}_{239}\text{H}_{196}$.¹⁰

In this paper, we present optical-absorption spectrum calculations of hydrogenated Si nanocrystallites in the range of 2.7–6.5 nm, to show the size effects in higher excited states, in order to provide a reference for experiments. The largest nanocrystallite calculated in this paper contains 13 464 silicon and 2730 hydrogen atoms, which is an order of magni-

tude larger than the nanocrystallites calculated in previous reports.^{8,9} An order N method is used for calculating linear-response functions for a large matrix, which is one of the most efficient methods in terms of both computational and memory requirements. This method is very general and can be applied in calculating optical-absorption spectra of any material systems such as amorphous, point defects, surface, or quasicrystals.

In the real-time real-space method, the complex dielectric function $\varepsilon_{\beta\alpha}(\omega)$ is given by¹¹

$$\varepsilon_{\beta\alpha}(\omega) = 1 + 4\pi \left\langle \left\langle \int_0^T dt e^{-\eta t} (e^{i\omega t} - \delta_{\beta\alpha}) K_{\beta\alpha}(t) \right\rangle \right\rangle \quad (1)$$

and

$$K_{\beta\alpha}(t) = \frac{-2}{V(\omega + i\eta)^2} \text{Im} \langle \Phi | \theta(E_F - H) e^{iHt} \times p_\beta e^{-iHt} \theta(E_{\text{cut}} - H) \theta(H - E_F) p_\alpha | \Phi \rangle, \quad (2)$$

where $\alpha, \beta = x, y, z$ and H, p_α, E_F, V , and $\theta(H)$ are the Hamiltonian of the system, the momentum operator, the Fermi energy, the volume of the system, and a step function, respectively. V is defined by $V = a_0^3 (N_{\text{Si}}/8)$, where a_0 and N_{Si} are the lattice constant and the number of Si atoms. T is set to satisfy $e^{-\eta T} < \delta$, where δ is a small number. Note here that both the real and the imaginary parts of the dielectric function are obtained, which is one of the advantages of our method. The total time T is proportional to the energy bandwidth divided by the energy resolution of the calculation η , which gives a Lorentzian width for each calculated transition. In Eq. (1), the trace is approximated with the statistical average over random phase vectors $|\Phi\rangle$ (Ref. 12) indicated by the double brackets, for which computational cost is $O(N)$. Here $|\Phi\rangle$ is a $N = N_x \times N_y \times N_z$ column vector for a system defined by a real-space uniform grid of $N_x \times N_y \times N_z$. The Hamiltonian is discretized in the real space by the higher-order finite difference method¹³ of the order 2.

In what follows, we consider hydrogenated silicon nanocrystallites and a bulk Si. The empirical pseudopotentials¹⁴ for silicon and hydrogen¹⁵ are used for the potential term in the Hamiltonian. The empirical pseudopotential method (EPM) requires more basis per atom as compared to tight-

binding methods by a factor of ≈ 50 . We choose to use EPM, however, because the purpose of the present paper is to calculate the absorption spectra in the higher states up to about 20 eV, where tight-binding methods^{10,16} fail to give a good approximation unless basis functions for describing higher bands are correctly taken into account.

First, the potential is constructed in the momentum space by a plane-wave expansion with the cutoff energy of 4.5 Ry in a grid of $N_x \times N_y \times N_z$. Then the potential is converted in the real space by a fast Fourier transformation (FFT). Since FFT is used only once in the calculation in obtaining the potential, the calculation time required for FFT is only a small portion of the total computation time. A boundary condition is applied such that the wave functions vanish outside the defined grids for hydrogenated Si nanocrystallites. The distance between hydrogen atoms and the boundary is taken to be larger than 0.7 nm. A periodic boundary condition is applied for a bulk Si.

The calculation Eq. (1) is performed by first calculating two vectors, $\theta(E_{\text{cut}}-H)\theta(H-E_F)p_\alpha|\Phi\rangle$ and $\theta(E_F-H)|\Phi\rangle$. $\theta(E_{\text{cut}}-H)$ is inserted for eliminating statistical fluctuations in calculated spectra originating from unphysical high-energy components. The most time consuming part of the calculation is the time evolutions of these vectors calculated by the leap frog method.¹⁷ One Hamiltonian-vector multiplication for each vector and one p_α multiplication are required for a single time evolution step. Since both H and p_α are sparse matrices, the computational cost for a time evolution step calculation is $O(N)$. The computational cost of the Fourier integral in Eq. (1), which is proportional to the total time steps, is negligible as compared to the above time evolution step calculation because the integrand in Eq. (1) is a scalar function of t . One of the most notable advantages of our method is a small memory requirement. The memory spaces required for the calculation are seven N -column vectors for storing vectors for the time evolutions and for a potential of the system. For example, only 319 megabytes are required for $N=144$, which can be fitted easily in the main memory of a computer; no disk storage is necessary. This requirement is significantly smaller than the Chebyshev polynomial expansion method.⁸

Figure 1 shows the density of states calculated by a time evolution method as given by

$$\rho(\omega) = -\frac{1}{\pi} \text{Im}\{\text{tr}[G(\omega + i\eta)]\}, \quad (3)$$

where $G(\omega + i\eta)$ is a real-time Green's function.¹¹ The density of states is calculated for cubic hydrogenated Si nanocrystallites of $\text{Si}_{1050}\text{H}_{498}$, $\text{Si}_{1632}\text{H}_{666}$, $\text{Si}_{4048}\text{H}_{1182}$, $\text{Si}_{8120}\text{H}_{1950}$, and $\text{Si}_{13464}\text{H}_{2730}$ with faces (110), (110), and (001). The density of states of bulk Si with 13 824 Si atoms is also calculated. The grids are varied from $72 \times 72 \times 72$ to $144 \times 144 \times 144$ and a total of 15 to 10 sets of initial random vectors are used, depending on the size of the nanocrystallites. Then the order of the largest Hamiltonian matrix H is $144^3 = 2\,985\,984$. The time steps and the total time T for the calculations are 1.37×10^{-18} s and 3.79×10^{-14} s. The energy resolution η and E_{cut} is set to be 80 meV and 50 eV, respectively. Calculated density of states inside the gap has artificial finite value, which originates from the accumulated

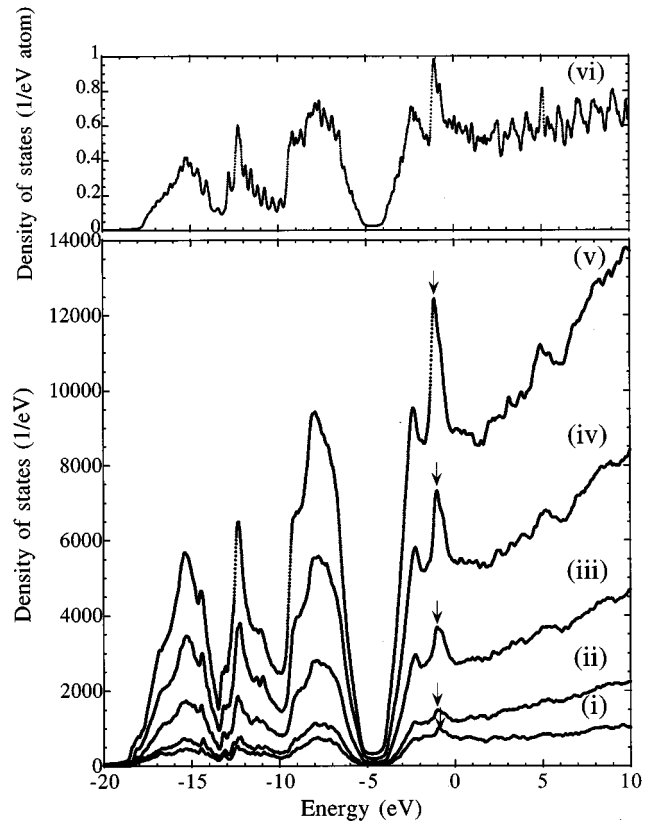


FIG. 1. Density of states of hydrogenated Si nanocrystallites (i) $\text{Si}_{1050}\text{H}_{498}$, (ii) $\text{Si}_{1632}\text{H}_{666}$, (iii) $\text{Si}_{4048}\text{H}_{1182}$, (iv) $\text{Si}_{8120}\text{H}_{1950}$, (v) $\text{Si}_{13464}\text{H}_{2730}$, and (vi) bulk Si with 13 824 Si atoms. One of the peaks in the conduction band is denoted by the arrows.

tails of Lorentzian distributions and can be made smaller by decreasing η . The peak between -0.93 and -1.2 eV shifts to higher energy with a decrease in size, as shown by the arrows in Fig. 1, while three major peaks in the valence bands do not show this high-energy shift within the accuracy of the calculations.

The size effect is more evident in the optical-absorption spectra of hydrogenated Si nanocrystallites and a bulk Si with 13 824 Si atoms. Figure 2 shows the calculated absorption coefficient spectra given by $K = 2\omega k/c$ with the complex refractive index defined by $n + ik = \epsilon^{1/2}$. Parameters used for the calculations of the absorption coefficient spectra are the same as those used for the calculations of the density of states, except for the number of sets of initial random vectors, which is between 4 and 7, depending on the size. The Coulomb interaction between an optically created electron-hole pair is known to give corrections in the energy region below about 3.5 eV. A general good agreement with the experiments is known to be achieved above 4 eV.¹⁴ In what follows, we focus on the structures above 4 eV, where the excitonic effect plays a smaller role. The structure around 4.5 eV, which is called the E_2 structure, is considered to be originating from the states around the special point $(2\pi/a_0)(\frac{3}{4}, \frac{1}{4}, \frac{1}{4})$ having M_2 symmetry in a bulk Si. The structure around 5.4 eV, which is called the E'_1 structure, is considered to be originating from the transition between L'_3 and L_1 , and transitions along L'_3 and L_3 , having M_0 and M_1 symmetry in a bulk Si.¹⁴

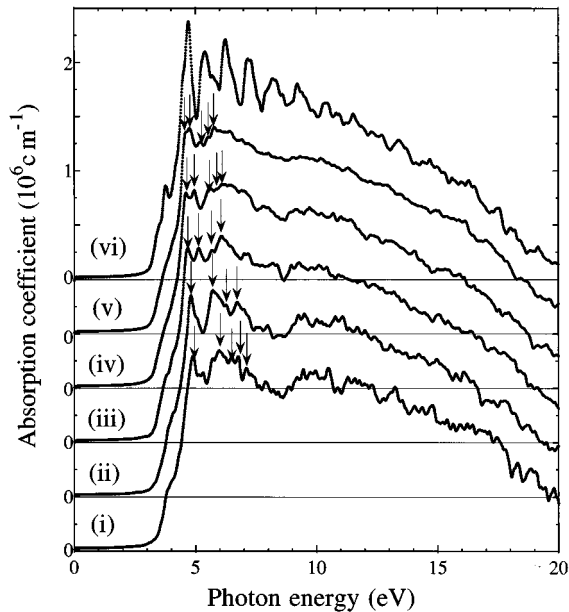


FIG. 2. Optical-absorption coefficient of hydrogenated Si nanocrystallites (i) $\text{Si}_{1050}\text{H}_{498}$, (ii) $\text{Si}_{1632}\text{H}_{666}$, (iii) $\text{Si}_{4048}\text{H}_{1182}$, (iv) $\text{Si}_{8120}\text{H}_{1950}$, (v) $\text{Si}_{13464}\text{H}_{2730}$, and (vi) bulk Si with 13 824 Si atoms. Zero points of the y axis are shifted as shown by the horizontal lines. Several peak positions are denoted by the arrows.

Figure 3 shows the size dependence of several peak positions, which are designated by arrows in Fig. 2. The lowest two peak positions are best fitted as $E = E_0 + C_0 L^{-\delta}$, with $\delta = 1.9$ in the size region of the present calculation larger than 2.7 nm, where L is the length of the side of the cube of silicon atoms. For the higher two or three peaks, the correlation of the peaks between different sizes of the nanocrystallites are less clear, as can be seen in Fig. 3. The deviations from the fitted curves are explained partly by the statistical fluctuations in the calculations. A smaller exponent of $\delta = 1.37$ was found for the band-gap energy in the size region below 3.7 nm.¹⁵ The coefficients C_0 are 2.7 and 9.4 (eV nm^{1.9}) for the two fitted curves in Fig. 3, respectively. The empirical scaling law of $L^{-1.9}$ deduced from Fig. 3 cannot be

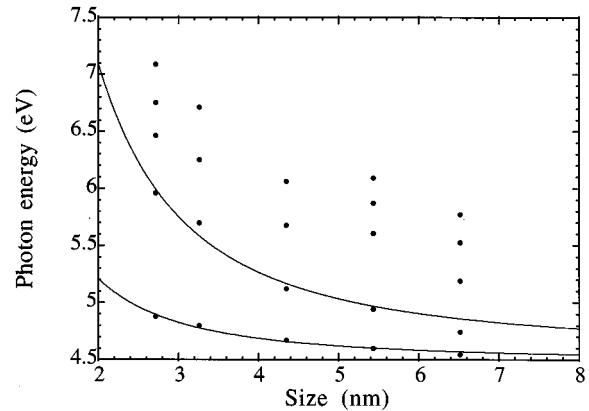


FIG. 3. Size dependence of peak positions in the calculated optical-absorption spectra and the best fitted curves.

directly comparable to $\delta = 1.37$ in the literature for the size dependence of the band gap. The exponent δ for the band gap is considered to be larger than 1.37 and closer to $\delta = 2$ in the size region larger than 3.7 nm. It would be interesting to construct an analytical theory to explain the size dependence of the peaks in the absorption spectra to compare with our result. Also, verification of our theory by experimental results is awaited.

In conclusion, the optical-absorption spectra of hydrogenated silicon nanocrystallites up to $\text{Si}_{13464}\text{H}_{2730}$ have been calculated by a linear scale calculation in real space, which is based on the time-dependent representation of a linear-response function. It is demonstrated that our method is efficient in terms of both computational and storage requirements. Our method is very general and can also be applied to other material systems. Size dependence of the optical-absorption peak positions between 4.5 and 6.0 eV is shown to be proportional to $L^{-1.9}$.

One of the authors (S.N.) appreciates computational support of the Computation Center RIKEN for providing CPU time of VPP-500. This work was partially supported by a Grant-in-Aid for Scientific Research of the Ministry of Education, Science, Sports, and Culture of Japan.

¹See, for example, *Porous Silicon Science and Technology*, edited by J.-C. Vial and J. Derrien (Springer and Les Edition de Physique, Berlin, 1995).

²H. Takagi *et al.*, *Appl. Phys. Lett.* **56**, 2379 (1990).

³K. A. Littau *et al.*, *J. Phys. Chem.* **97**, 1224 (1993).

⁴Y. Kanemitsu, T. Ogawa, K. Shiraishi, and K. Takeda, *Phys. Rev. B* **48**, 4883 (1993).

⁵S. Hayashi and K. Yamamoto, *J. Lumin.* **70**, 352 (1996).

⁶X. Zhao *et al.*, *Jpn. J. Appl. Phys., Part 2* **33**, L649 (1994).

⁷S. Nomura, X. Zhao, Y. Aoyagi, and T. Sugano, *Phys. Rev. B* **54**, 13 974 (1996).

⁸L. W. Wang, *Phys. Rev. B* **49**, 10 154 (1994).

⁹A. Zunger and L. W. Wang, *Appl. Surf. Sci.* **102**, 350 (1996).

¹⁰F. Huaxiang, Y. Ling, and X. Xide, *Phys. Rev. B* **48**, 10 978 (1993).

¹¹T. Iitaka *et al.*, *Phys. Rev. E* **56**, 1222 (1997).

¹²O. F. Sankey, D. A. Drabold, and A. Gibson, *Phys. Rev. B* **50**, 1376 (1994).

¹³J. Chelikowsky, N. Troullier, and Y. Saad, *Phys. Rev. Lett.* **72**, 1240 (1994).

¹⁴M. L. Cohen and J. R. Chelikowsky, *Electronic Structure and Optical Properties of Semiconductors*, 2nd ed. (Springer-Verlag, Berlin, 1988).

¹⁵L. W. Wang and A. Zunger, *J. Chem. Phys.* **100**, 2394 (1994).

¹⁶A. Voter, J. Kress, and R. Silver, *Phys. Rev. B* **53**, 12 733 (1996).

¹⁷T. Iitaka, *Phys. Rev. E* **49**, 4684 (1994).